Zero : Jurnal Sains, Matematika, dan Terapan
E-ISSN : 2580-5754; P-ISSN : 2580-569X
Volume 10, Number 2, 2026
DOI: 10.30829/zero.v10i2.28837
Page: 535-548

Sector-Adjusted R-vine Copula (RVMS) Extension of CAPM for Portfolio Risk Optimization

[1]Wa Ode Intan Fully Nadya
School of Data Science, Mathematics, and Informatics, IPB University, Bogor, Indonesia

[2]Retno Budiarti
School of Data Science, Mathematics, and Informatics, IPB University, Bogor, Indonesia

[3]I Gusti Putu Purnaba
School of Data Science, Mathematics, and Informatics, IPB University, Bogor, Indonesia

Article Info

Article history:

Accepted: 10 July 2026

Keywords:

CAPM;
Copula;
Optimization;
Portfolio;
R-vine.

ABSTRACT

This study evaluated the R-vine Market Sector (RVMS) model, a sector-adjusted extension of the Capital Asset Pricing Model (CAPM), for portfolio risk optimization in the Indonesian stock market using 978 daily observations from 2021 to 2025. Returns were modeled using ARMA GARCH and R-vine copulas, and portfolios were optimized under a minimum tail-risk criterion with rolling-window backtesting. The results indicated asymmetric and tail dependence, with sectoral effects contributing substantially to portfolio risk. RVMS reduced expected tail losses by approximately 12–16% relative to CAPM at standard confidence levels, although both models showed limited performance under extreme tail conditions. Economically, RVMS provided modest improvements in risk-adjusted performance and lower drawdowns, despite higher turnover. Overall, incorporating sectoral dependence improved portfolio risk modeling, although the benefits remained moderate and context-dependent.

Corresponding Author:

Wa Ode Intan Fully Nadya,
Department of Applied Mathematics
IPB University, Bogor, Indonesia
Email: intanfully@apps.ipb.ac.id

1. INTRODUCTION

A robust understanding of asset valuation and risk management is essential for effective portfolio allocation, particularly amid increasing global market volatility. Recent extreme shocks, including the COVID-19 pandemic and geopolitical conflicts in the Middle East, have highlighted the susceptibility of financial markets to simultaneous extreme movements across assets. These conditions emphasize an urgent need for advanced risk management approaches capable of capturing complex multivariate dependence, particularly joint tail behavior. This challenge is especially relevant in emerging markets such as Indonesia, where higher volatility and information asymmetry prevail. As a result, conventional portfolio risk models may produce biased estimates of Value-at-Risk (VaR) and Expected Shortfall (ES), especially during stress periods [1].

The Capital Asset Pricing Model (CAPM) remains one of the most widely used frameworks for measuring systematic risk through the beta coefficient [2], [3], [4]. However, CAPM relies on linear dependence and normality assumptions that limit its ability to capture nonlinear interactions and tail dependence frequently observed in financial markets, particularly in emerging economies with volatile and heterogeneous market behavior [3], [4], [5], [6], [7], [8], [9], [10]. Consequently, more flexible dependence modeling approaches are required to improve portfolio risk estimation under extreme market conditions.

To address these limitations, copula-based approaches have increasingly been adopted to model nonlinear and asymmetric dependence structures among financial assets [11], [12], [13]. Among these, vine copula models provide a particularly flexible framework for high-dimensional dependence modeling through pairwise copula decompositions, enabling more accurate representation of tail dependence and complex inter-asset relationships [14], [15], [16]. Previous studies have demonstrated that vine copula approaches improve portfolio risk estimation and enhance the modeling of extreme co-movements, especially during periods of financial turbulence [17], [18], [19]. Furthermore, when integrated with ARMA-GARCH models, vine copulas are capable of jointly capturing marginal return dynamics and multivariate dependence structures, making them suitable for portfolio-level risk assessment and stress testing [1], [20]. These developments have motivated the emergence of several vine-based extensions designed to overcome the restrictive assumptions of traditional asset pricing frameworks.

One such extension is the Canonical Vine Autoregressive (CAVA) model, which was introduced to relax the restrictive assumptions of CAPM [21]. Based on a C-vine structure, CAVA assumes a single dominant factor—typically the global market—as the central conditioning variable governing all pairwise dependencies. Although this framework provides greater flexibility than conventional linear models, it still imposes a relatively homogeneous dependence structure driven by one dominant factor. Consequently, the model may be limited in capturing sector-specific interactions and heterogeneous dependence patterns across assets, particularly during periods of market disruption when sectoral responses become increasingly differentiated.

To address this limitation, the R-vine Market Sector (RVMS) model adopts a Regular vine (R-vine) topology that allows multiple conditioning variables organized through sector-based groupings. Unlike the centralized star-shaped structure of CAVA, the RVMS framework transforms the dependence structure into a hierarchical network of sector-conditioned pair-copulas. This flexibility enables the model to capture cross-sectional heterogeneity, asymmetric dependence, and sector-driven interactions that become more pronounced during global and sectoral shocks. The R-vine structure, which does not rely on a single dominant node, has also been shown to outperform alternative dependence models in capturing extreme co-movements, including during the COVID-19 crisis [22]. By explicitly incorporating sectoral effects, RVMS provides a more comprehensive representation of both market-wide and sector-specific risks [5].

Despite its theoretical advantages, empirical applications of sector-conditioned R-vine copula models in emerging markets remain limited. Existing studies often treat dependence modeling, tail-risk estimation, and portfolio optimization separately, with limited integration into a unified framework. Moreover, sector-based hierarchical dependence structures within R-vine copulas remain underexplored, particularly in the Indonesian stock market context [23]. These limitations highlight the need for an integrated framework capable of simultaneously modeling sector-conditioned dependence structures and tail-risk-based portfolio optimization in emerging markets. Accordingly, this study contributes to the literature in several key aspects:

a. Theoretical Contribution: extends dependence modeling by introducing a sector-conditioned hierarchical structure within an R-vine framework, relaxing the single-factor assumption of CAVA.
b. Methodological Contribution: develops the RVMS model for portfolio optimization by integrating multivariate dependence modeling with Conditional Value-at-Risk (CVaR) as a tail-risk measure.
c. Empirical Contribution: provides empirical evidence from the Indonesian stock market, demonstrating the benefits of sector-aware dependence modeling in improving portfolio performance and risk mitigation.

The novelty of this study lies in integrating sector-based hierarchical dependence within a flexible R-vine copula framework for portfolio optimization under tail-risk considerations. Therefore, this study aims to develop and evaluate the RVMS model to assess whether it enhances tail-risk estimation and portfolio performance relative to conventional approaches.

2. RESEARCH METHOD

2.1 Data and Tools

2.1.1 Data Sources and Selection

This study employs secondary data consisting of daily adjusted closing prices obtained from Investing.com, Yahoo Finance, and the Indonesia Stock Exchange (IDX). Adjusted prices were used to account for corporate actions such as dividends, stock splits, and rights issues. The dataset includes the Jakarta Composite Index (IHSG/JKSE), two sectoral indices (JKFINANCE and JKENERGY), and four large-cap stocks: BBCA, BBRI, ADRO, and PGAS. The observation period spans from June 2021 to June 2025, comprising 978 observations and covering the post-pandemic recovery and recent global market fluctuations.

2.1.2 Data Preprocessing and Validation

Prior to analysis, preprocessing procedures were applied to ensure data consistency and integrity. Missing observations were handled using an intersection approach without interpolation, and all series were temporally synchronized. Corporate action adjustments were cross-validated across data sources, while the mean absolute difference in daily log-returns remained below 0.02%, indicating negligible discrepancies in the dataset.

2.1.3 Return Calculation and Software

Returns are calculated as continuously compounded (logarithmic) returns, defined as:

$$r_t = \ln\left(\frac{P_t}{P_{t-1}}\right) \tag{1}$$

where P_t and P_{t-1} denote the adjusted closing prices at time t and $t-1$, respectively. The use of log-returns ensures statistical stability and is standard in financial econometrics. For CAPM-based analysis, excess returns are computed by adjusting asset returns with the risk-free rate. The risk-free rate is proxied by the Indonesian government bond yield (approximately 6.4% annually) and converted into daily frequency assuming 252 trading days. This proxy is chosen as it represents a tradable, low-risk asset consistent with CAPM assumptions.

All computations are performed using R version 4.5.1 on a Windows 11 platform. The analysis utilizes several packages, including VineCopula for dependence modeling, rugarch for marginal volatility modeling, PortfolioAnalytics for portfolio optimization, and PerformanceAnalytics for risk evaluation. The specification of software and packages ensures the reproducibility of the empirical results.

2.2 Research Procedures

The research procedure consisted of seven main stages: data exploration, CAPM estimation (benchmark), marginal modelling, dependence modelling (RVMS), dependence-based risk analysis, portfolio optimization, and backtesting model. A detailed explanation of these steps is provided below.

a. Data Exploration

Descriptive statistics and graphical analysis were conducted to examine distributional characteristics. Time series plots and histograms are used to visualize distributional patterns and identify potential outliers. Normality was assessed using the Jarque–Bera (JB), Anderson–Darling (AD), and Shapiro–Wilk (SW) tests. For notational consistency, the log-return series were denoted as r_t^M for the market index (IHSG), r_t^F for the financial sector index (JKFINANCE), r_t^E for the energy sector index (JKENERGY), and $r_{1,t}^F, r_{2,t}^F, r_{1,t}^E, r_{2,t}^E$ for individual assets corresponding to BBCA, BBRI, ADRO, and PGAS, respectively.

b. CAPM Estimation (Benchmark)

The systematic risk of each asset was estimated using the CAPM. The beta coefficient was computed as:

$$\beta_i^s = \frac{\mathrm{Cov}(r_{i,t}^s, r_t^M)}{\mathrm{Var}(r_t^M)}, \text{with } s \in \{F, E\} \tag{2}$$

where $r_{i,t}^s$ denotes the excess log-return of asset i in sector s and r_t^M represents the excess log-return of the market index, both computed relative to the risk-free rate. Based on this, the total risk of each asset was decomposed into systematic ($\beta_i^2\mathrm{Var}(r_t^M)$) and non-systematic ($\mathrm{Var}(\varepsilon_{i,t}^s)$) components as [5]:

$$\mathrm{Var}(r_{i,t}^s) = (\beta_i^s)^2\mathrm{Var}(r_t^M) + \mathrm{Var}(\varepsilon_{i,t}^s) \tag{3}$$

c. Marginal Modelling

The marginal modeling stage aims to remove serial dependence and heteroscedasticity from the log-return series, producing residuals that are approximately independently and identically distributed (i.i.d.). Each series was tested for stationarity using the ADF test and for conditional heteroscedasticity using the ARCH–LM test [24]. Autocorrelation structures were examined using ACF and PACF plots. When serial dependence was detected, an ARMA(p,q) model was fitted, expressed as [25]:

$$r_{i,t}^s = \mu_i^s + \sum_{j=1}^{p} \phi_{i,j}^s r_{i,t-j}^s + \varepsilon_{i,t}^s + \sum_{k=1}^{q} \theta_{i,k}^s \varepsilon_{i,t-k}^s \tag{4}$$

where p and q represent the orders of the AR and MA processes, respectively. Model parameters were estimated using Maximum Likelihood Estimation (MLE), and residual diagnostics were conducted using the Ljung–Box test to ensure white noise properties.

A range of GARCH-type models was estimated to capture volatility clustering and asymmetry, including sGARCH, eGARCH, and GJR-GARCH models with normal, Student-t, and skewed Student-t distributions. Volatility clustering refers to the persistence of high- and low-volatility periods in financial time series [26]. The standard GARCH (p,q) model was defined as follows [25][27]:

$$\sigma_t^2 = \omega + \sum_{j=1}^{q} \alpha_j \varepsilon_{t-j}^2 + \sum_{k=1}^{p} \beta_k \sigma_{t-k}^2 \tag{5}$$

where σ_t^2 denotes the conditional variance. The optimal model was selected based on the Akaike Information Criterion (AIC), subject to residual diagnostic tests confirming the absence of remaining ARCH effects and serial correlation. Let σ_t^2 denote the conditional variance obtained from the selected GARCH-type model. The standardized residuals were then computed as:

$$z_{i,t}^s = \frac{\varepsilon_{i,t}^s}{\sigma_{i,t}^s} \tag{8}$$

where $\varepsilon_{i,t}^s$ denotes the innovation (error) term. The standardized residual vector $\boldsymbol{Z}_t = \left(z_{1,t}^s, \dots, z_{N,t}^s\right)$ was subsequently transformed into uniformly distributed variables using the probability integral transform (PIT):

$$u_{i,t}^s = F_i^s\left(z_{i,t}^s\right), \qquad u_{i,t}^s \sim \text{Uniform } (0,1), \tag{9}$$

where $F_i^s(.)$ denotes the fitted marginal distribution for asset i in sector s. The transformed variables were then used to construct the RVMS copula model.

d. Dependence Modelling (RVMS)

The joint dependence structure was modeled using the RVMS copula based on the R-vine framework. The hierarchical structure reflected market–sector–asset relationships, where the first tree captured dependencies between assets and sectors as well as sectors and the market, while the second tree modeled asset–market dependencies conditional on sectoral effects. Let $\mathbf{u}_t = \left\{u_{1,t}^s, \dots, u_{d,t}^s\right\}$ denote the vector of transformed uniform variables at time t, where each component $u_{i,t}^s \in (0,1)$ is obtained via the probability integral transform (PIT) applied to the standardized residuals. The multivariate copula density was decomposed into a product of bivariate copulas as [5]:

$$c(\mathbf{u}_t) = \prod_{m=1}^{d-1} \prod_{e \in E_m} c_{j_e,k_e}|D_e \left(u_{j_e}|D_e, u_{k_e}|D_e\right), \tag{10}$$

where $u_{j_e}|D_e$ and $u_{k_e}|D_e$ represent conditional distribution functions obtained through the h-functions associated with the vine copula structure.

Several copula families, including Gaussian, Student-t, Clayton, Gumbel, and Frank copulas, were evaluated for the first and second trees. The optimal pair-copula was selected using the Akaike Information Criterion (AIC). For higher-order trees, Gaussian copulas were employed to improve estimation stability and computational efficiency, as higher-order conditional dependencies are generally weaker and more difficult to estimate reliably [5]. The simplified RVMS specification was subsequently compared with a fully flexible vine copula model using the AIC.

Kendall's tau (τ) was used as the dependence measure, and pair-copula parameters were estimated using Maximum Likelihood Estimation (MLE). To capture extreme co-movements, lower (λ^L) and upper (λ^U) tail dependence coefficients were also computed as [28]:

$$\lambda^L = \lim_{u \to 0^+} \frac{C(u,u)}{u} \text{ and } \lambda^U = \lim_{u \to 1} \frac{1-2u+C(u,u)}{1-u} \tag{11}$$

where $C(u,u)$ denotes the copula cumulative distribution function corresponding to the selected pair-copula.

e. Dependence-Based Risk Analysis

The RVMS framework was employed to analyze the dependence structure of asset returns and to provide a proxy for decomposing portfolio risk into sectoral, conditional sector–market, and non-systematic components. Let $\tau_{i,j}$ denote the Kendall's tau associated with each pair-copula between variables i and j.

Specifically, $\tau_{i,s}$ represents the dependence between asset i and its corresponding sector, while $\tau_{i,M|s}$ denotes the conditional dependence between asset i and the market given the sector. Following Brechmann and Czado [5], this decomposition should be interpreted as a dependence-based allocation heuristic rather than an exact variance decomposition, since Kendall's tau measures dependence intensity rather than marginal risk contribution. The relative sectoral dependence contribution is defined as [5]:

$$R_{i,s} = \frac{|\tau_{i,s}|}{\sum_{j \in D_i} |\tau_{i,j}|} \tag{12}$$

Similarly, the conditional sector–market contribution is given by:

$$R_{i,M|s} = \frac{|\tau_{i,M|s}|}{\sum_{j \in D_i} |\tau_{i,j}|} \tag{13}$$

where D_i denotes the set of all pairwise dependence terms associated with asset i in the vine structure. Absolute values are used to avoid cancellation between positive and negative dependence measures. The resulting weights are normalized such that the decomposition sums to one for each asset. The non-systematic component is then defined residually as:

$$R_{i,\varepsilon} = 1 - (R_{i,s} + R_{i,M|s}) \tag{14}$$

The sum $R_{i,s}$ and $R_{i,M|s}$ is interpreted as the systematic component, while the non-systematic component captures the remaining higher-order dependencies beyond the primary sectoral and conditional market relationships. Accordingly, the resulting quantities represent relative dependence intensities rather than variance-based risk contributions.
To complement the Kendall's tau analysis, a sensitivity analysis was conducted using lower and upper tail dependence coefficients derived from the estimated copula parameters. Using the same normalization framework, the decomposition was performed separately for lower and upper tails to evaluate dependence behavior under extreme negative and positive market conditions. Differences between the two decompositions indicate the influence of extreme events on the dependence structure and resulting allocation.

f. Portfolio Optimization

Next, portfolio return simulations were conducted using the fitted RVMS model. The simulation procedure began by generating a vector of independent random variables:

$$v_{i,t} \sim \text{Uniform } (0,1), \quad i = 1, \dots, d \tag{15}$$

These independent uniform variables are transformed into dependent uniform variables $u_{i,t}^s$ using the inverse Rosenblatt transform based on the fitted R-vine copula structure. The transformation is performed sequentially, where the i-th component is given by [29]:

$$u_{i,t}^s = F_{i|1,\dots,i-1}^{-1}\left(v_{i,t}; u_{1,t}^s, \dots, u_{i-1,t}^s\right), i = 1, \dots, d \text{ with } u_{1,t}^s = v_{1,t} \tag{16}$$

where $F_{i|1,\dots,i-1}^{-1}(.)$ denotes the inverse conditional distribution function derived from the corresponding pair-copulas. The resulting uniform variables were then transformed into standardized residuals using the inverse cumulative distribution function:

$$z_{i,t}^s = (F_i^s)^{-1}\left(u_{i,t}^s\right), \tag{17}$$

where F_i^s denotes the cumulative distribution function of the selected marginal distribution for asset i in sector s. Simulated returns were subsequently obtained using the conditional mean and volatility from the fitted GARCH-type models:

$$r_{i,t}^{s,*} = \mu_{i,t}^{s,*} + \sigma_{i,t}^s z_{i,t}^s \tag{18}$$

Let $r_t = (r_{1,t}^{s,*}, \dots, r_{N,t}^{s,*})$ denote the vector of simulated asset returns at scenario t. was performed using the minimum Conditional Value-at-Risk (CVaR) criterion for both the CAPM and RVMS frameworks [30][31][32]. The portfolio loss under scenario t is defined as:

$$L_t = -\mathbf{w}^{\mathrm{T}} r_t \tag{19}$$

where $\mathbf{w}^{\mathrm{T}} = (w_1, \dots, w_N)$ the transpose of vector $\mathbf{w}$. The excess loss variable is given by:

$$x_t = \max(0, L_t - \eta) \tag{20}$$

assuming all simulated scenarios are equally weighted, each scenario is assigned a probability weight of $\frac{1}{q}$, where q is the total number of simulated observations and η represents the Value-at-Risk (VaR). Following the linear programming reformulation of CVaR based on the sample average approximation proposed by Rockafellar and Uryasev [32], the optimization problem can be expressed as:

$$\begin{gathered}
\min_{w,\eta,x_t} \eta + \frac{1}{(1-\alpha)q} \sum_{t=1}^{q} x_t \\
\text{s.t } x_t \geq -\mathbf{w}^{\mathrm{T}} r_t - \eta, \; t = 1, \dots, q \\
x_t \geq 0, \\
\sum_{i=1}^{N} w_i = 1, \\
0.1 \leq w_i \leq 0.4, \qquad i = 1, \dots, N.
\end{gathered}$$

where $w_i = (w_1, \dots, w_N)$ the portfolio weights and α denotes the confidence level.
The optimization was conducted under fully invested and bound constraints, with portfolio weights restricted between 0.1 and 0.4 to promote diversification and avoid excessive concentration. To account for estimation uncertainty, bootstrap resampling with 1,000 replications was applied to the simulated portfolio returns. CVaR was re-estimated at the 95% and 99% confidence levels, and the resulting bootstrap distribution was used to compute standard errors and 95% confidence intervals using the percentile method.

g. Backtesting Model

Finally, the performance of the model was evaluated through a rolling-window backtesting procedure. At each time step, the model was re-estimated using a fixed rolling window of 300 trading days. This re-estimation involves fitting the marginal GARCH models, constructing the R-vine copula for dependence modeling, generating Monte Carlo simulations, and performing CVaR-based portfolio optimization. One-step-ahead out-of-sample portfolio returns were then computed using the optimized weights. The portfolio was rebalanced on a daily basis, consistent with the refitting frequency applied in the rolling scheme. The out-of-sample evaluation period consists of $T - 300 - 1$ observations (i.e., 677 out-of-sample forecasts), corresponding to all available observations following the initial 300-day estimation window and one-step-ahead forecasting scheme, where T denotes the total sample size. The resulting series of VaR and Expected Shortfall (ES) forecasts were evaluated using the Kupiec test to assess unconditional coverage [5], the Christoffersen test to examine conditional coverage and the independence of violations [33], and the McNeil–Frey test to validate the Expected Shortfall estimates [34]. In addition to statistical backtesting, the economic performance of the resulting portfolios was also evaluated using the out-of-sample return series. Specifically, the Sharpe ratio was employed to assess risk-adjusted returns, maximum drawdown was used to measure downside risk exposure, and portfolio turnover was calculated to capture the intensity of rebalancing and potential transaction costs. This complementary evaluation allows for a direct comparison between statistical risk accuracy and practical portfolio performance.

3. RESULT AND ANALYSIS

3.1 Data Exploration

The study commenced with descriptive statistical analysis to characterize each dataset. This analysis involved inspecting distributional patterns through plots and histograms and calculating the mean, standard deviation, skewness, kurtosis, and the extreme values (minimum and maximum). The corresponding plots and histograms are shown in the following Figure 1.

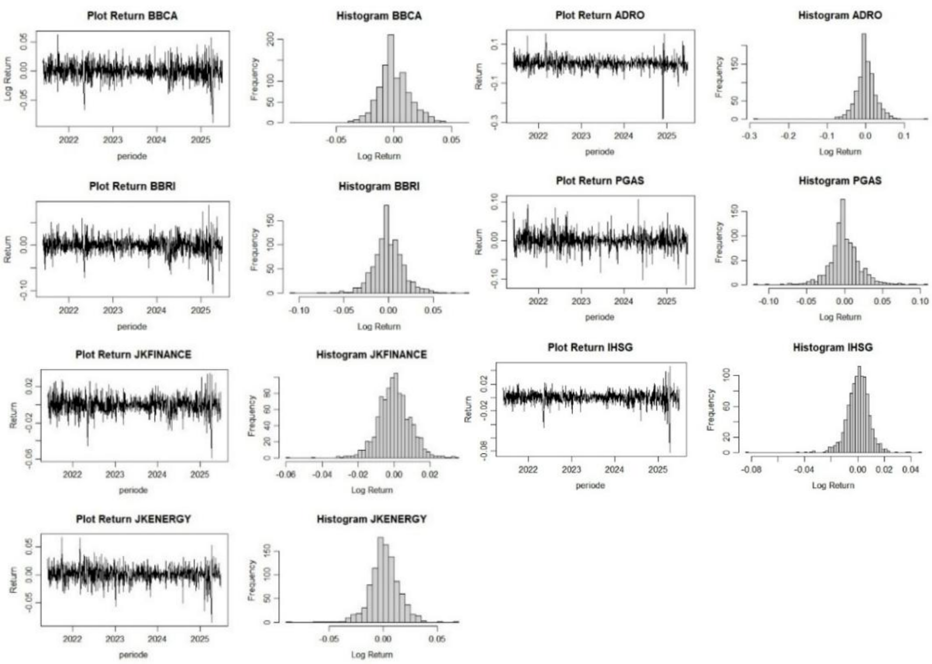

Figure 1. Plot and Histogram Time Series

The log-return plots revealed volatility clustering across all series, supporting the use of GARCH-type models. The histograms also indicated leptokurtic and fat-tailed behavior, implying that extreme returns occurred more frequently than expected under normality. These findings suggested that heavy-tailed distributions such as the student-t and skewed Student-t distributions were more appropriate for risk modeling.

Table 1. Descriptive Statistical Analysis

Statistic	r_t^M	r_t^F	r_t^E	$r_{1,t}^F$	$r_{2,t}^F$	$r_{1,t}^E$	$r_{2,t}^E$
Mean	0.000152	0.000027	0.001323	0.000312	-0.000084	0.000417	0.000337
Std. Deviasi	0.008872	0.009398	0.014069	0.014339	0.017926	0.029698	0.021176
Skewness	-0.978012	-0.240501	-0.213705	-0.088077	-0.102991	-1.336723	0.082805
Kurtosis	12.866223	5.644760	6.364839	5.787556	5.972302	21.700030	6.557939
Minimum	-0.082319	-0.059023	-0.085436	-0.089153	-0.106733	-0.284961	-0.115134
Maximum	0.046814	0.035389	0.067446	0.061875	0.088251	0.152908	0.107631

Based on the histogram and descriptive statistical analysis, the data used in this study were suspected to be non-normally distributed. To formally assess normality, the Jarque–Bera (JB), Anderson–Darling (AD), and Shapiro–Wilk (SW) tests were conducted. The results from all three tests indicated that all the data set did not follow a normal distribution.

3.2 CAPM Estimation (Benchmark)

The CAPM framework was used as a benchmark to assess the systematic risk of each asset relative to the market. Beta coefficients were estimated to capture the sensitivity of asset returns to market movements, and total risk was decomposed into systematic and non-systematic components. The estimation is based on excess returns computed using the risk-free rate proxy. The results of the beta estimation and risk decomposition are summarized in following tables.

Table 2. Estimated CAPM Beta Coefficients and Risk Decomposition

Assets	Beta ($\boldsymbol{\beta_i}$)	Systematic Risk	Non-Systematic Risk	Total Risk
$r_{1,t}^F$	1.019383	39.78%	60.22%	100%
$r_{2,t}^F$	1.329136	43.27%	56.73%	100%
$r_{1,t}^E$	1.182033	12.47%	87.53%	100%
$r_{2,t}^E$	0.764138	10.25%	89.75%	100%

The CAPM beta estimates in Table 2 indicated heterogeneous market sensitivities, with BBCA, BBRI, and ADRO exhibiting beta values greater than one, whereas PGAS showed lower systematic risk exposure. The decomposition results further indicated that asset risk was dominated by non-systematic rather than market-wide factors, particularly for ADRO and PGAS.

3.3 Marginal Modelling

The RVMS framework was employed to model dependence among the market, sectors, and assets. Marginal modeling involved stationarity, autocorrelation, and ARCH effect testing to determine appropriate ARMA–GARCH specifications. The ADF test confirmed that all series were stationary in the mean, while the ACF and PACF plots were used to determine the ARMA orders (*p,q*). The corresponding plots are presented in Figure 2.

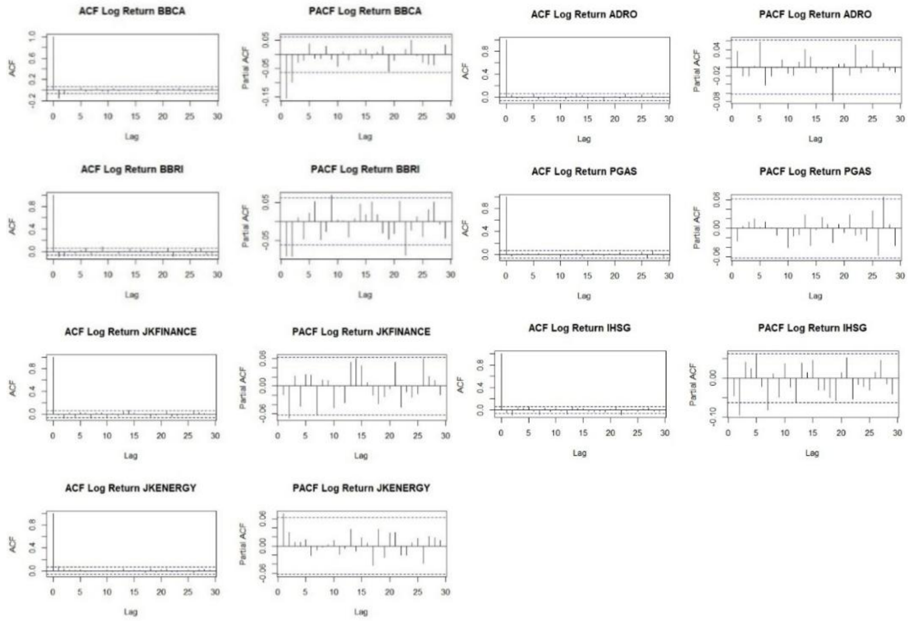

Figure 2. The ACF and PACF plots

The Ljung–Box test was also conducted to statistically examine autocorrelation. The results at lags 1 and 5 indicated the presence of autocorrelation in IHSG, JKENERGY, BBCA and BBRI, whereas JKFINANCE, ADRO dan PGAS showed no significant autocorrelation. The selected ARMA orders and corresponding parameter estimates are presented as follows.

Table 3. ARMA (*p,q*) Model Selection

Data	ARMA Order (p,q)	AR Coefficients ϕ	MA Coefficients θ
r_t^M	(0,3)	-	$\theta_1 = -0.0513, \theta_2 = -0.0889, \theta_3 = 0.0644$
r_t^F	(0,0)	-	-
r_t^E	(1,0)	0.0718	0
$r_{1,t}^F$	(0,2)	-	$\theta_1 = -0.1730, \theta_2 = -0.0728$
$r_{2,t}^F$	(0,2)	-	$\theta_1 = -0.0965, \theta_2 = -0.0856$
$r_{1,t}^E$	(0,0)	-	-
$r_{2,t}^E$	(0,0)	-	-

The Ljung–Box and ARCH–LM tests were conducted to verify the white noise assumption of the ARMA residuals. The results showed no significant autocorrelation across all series. However, only PGAS produced an ARCH–LM p-value greater than 0.05, indicating the absence of ARCH effects. Therefore, PGAS residuals were directly used in the RVMS structure, while the remaining series were modeled using GARCH-type models. The selected models are presented below.

Table 4. GARCH-Type Selection and Residual Distribution

Data	Model	Residual Distribution
r_t^M	eGARCH (1,1)	Skewed Student-t
r_t^F	eGARCH (1,1)	Student-t
r_t^E	GARCH (1,1)	Student-t
$r_{1,t}^F$	GJR-GARCH (1,1)	Skewed Student-t
$r_{2,t}^F$	eGARCH (1,1)	Student-t
$r_{1,t}^E$	GARCH (1,1)	Skewed Student-t

As shown in Table 4, the selected models indicated heterogeneous volatility dynamics across series. IHSG, JKFINANCE, and BBRI were best fitted by eGARCH (1,1), JKENERGY and ADRO by GARCH (1,1), and BBCA by GJR-GARCH (1,1), reflecting asymmetric and leverage effects. Most series were also better fitted by Student-t and skewed Student-t distributions, consistent with the fat-tailed behavior of the return series. The standardized residuals ($z_{i,t}^s$) were subsequently transformed into uniformly distributed variables $u_{i,t}^s$~Uniform (0,1) using the Probability Integral Transform (PIT).

3.4 Dependence Modelling (RVMS)

The uniformly distributed variables $u_{i,t}^s$~Uniform (0,1), obtained from the Probability Integral Transform (PIT), were used to construct the RVMS copula model. The estimated RVMS structure, along with the corresponding parameters and dependence measures, is presented in the following figure.

```
tree            edge | family  cop    par   par2 |   tau   utd   ltd
---------------------------------------------------------------------
   1             2,5 |      2    t   0.66   7.23 |  0.46  0.23  0.23
                 2,4 |      2    t   0.59   9.35 |  0.40  0.13  0.13
                 1,2 |      2    t   0.79   6.51 |  0.58  0.37  0.37
                 3,6 |      2    t   0.69   6.65 |  0.49  0.27  0.27
                 3,1 |      2    t   0.55   8.00 |  0.37  0.14  0.14
                 7,3 |      2    t   0.50  11.37 |  0.33  0.06  0.06
   2           1,5;2 |     14   SG   1.12   0.00 |  0.11     -  0.15
               1,4;2 |      1    N   0.23   0.00 |  0.15     -     -
               3,2;1 |      1    N  -0.24   0.00 | -0.16     -     -
               1,6;3 |      5    F  -0.24   0.00 | -0.03     -     -
               7,1;3 |     14   SG   1.05   0.00 |  0.05     -  0.06
   3         4,5;1,2 |      1    N   0.07   0.00 |  0.04     -     -
             3,4;1,2 |      1    N  -0.11   0.00 | -0.07     -     -
             7,2;3,1 |      1    N   0.04   0.00 |  0.02     -     -
             7,6;1,3 |      1    N  -0.03   0.00 | -0.02     -     -
   4       3,5;4,1,2 |      1    N  -0.08   0.00 | -0.05     -     -
           7,4;3,1,2 |      1    N  -0.00   0.00 | -0.00     -     -
           6,2;7,3,1 |      1    N  -0.02   0.00 | -0.01     -     -
   5     7,5;3,4,1,2 |      1    N   0.08   0.00 |  0.05     -     -
         6,4;7,3,1,2 |      1    N   0.02   0.00 |  0.01     -     -
   6   6,5;7,3,4,1,2 |      1    N   0.07   0.00 |  0.04     -     -
---
type: R-vine    logLik: 1741.58    AIC: -3429.17    BIC: -3297.26
---
1 <-> U_IHSG,   2 <-> U_JKFINANCE,   3 <-> U_JKENERGY,   4 <-> U_BBCA,
5 <-> U_BBRI,   6 <-> U_ADRO,   7 <-> U_PGAS
```

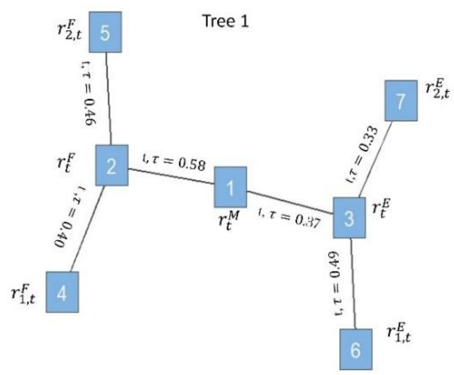

Figure 3. RVMS Structure

In Tree 1, the student-t copula was selected for all pair-copulas, indicating strong tail dependence across the primary relationships. The strongest dependence was observed for IHSG–JKENERGY, followed by IHSG–PGAS and JKFINANCE–BBCA, suggesting moderate to strong co-movements among the market, sectors, and assets. The presence of non-zero tail dependence further indicated that extreme market conditions may trigger simultaneous large asset movements. The estimated copula parameters (ρ, υ) were subsequently used to compute lower (λ^L) and upper (λ^U) tail dependence coefficients.

In Tree 2, conditional dependencies weakened sustantially. For example, the conditional dependence between JKFINANCE and BBCA given IHSG decreased to $\tau = 0.11$, while several other pairs exhibited very low or near-zero dependence. Similarly, the dependence between JKENERGY and ADRO became negligible after conditioning, despite exhibiting relatively strong dependence in Tree 1 ($\tau = 0.37$). These results suggested that much of the observed dependence was explained by common market and sectoral effects.

In higher-order trees (Trees 3–6), all pair-copulas were modeled using the Gaussian copulas, with Kendall's tau values close to zero, indicating weak conditional dependence. However, additional diagnostics using a fully flexible RVMS specification showed that several higher-order pairs were better fitted by non-Gaussian copulas, including Clayton and survival Gumbel copulas, indicating the presence of residual asymmetric and tail-dependent structures. Consistent with this finding, the fully flexible model produced a lower AIC value (−3461.82) than the simplified specification (−3429.17), indicating improved model fit. These results suggested that the Gaussian simplification may omit relevant dependence information, even when overall dependence strength is weak. Nevertheless, following Brechmann and Czado [5], the simplification remained a practical trade-off between model flexibility, estimation stability, and computational efficiency.

3.5 Dependence-Based Risk Analysis

The dependence-based decomposition results obtained from the RVMS framework are presented in Table 5. The results indicated that sectoral dependence dominated across all assets, confirming that return co-movements were primarily driven by sector-specific dynamics. Conditional market dependence remained weaker after controlling for sectoral effects (4.45%–21.97%), with the highest contribution observed for BBCA. The non-systematic component (15%–25%) also remained relevant, reflecting firm-specific and higher-order dependencies. Overall, sectoral and market factors explained most of the dependence structure.

Table 5. Dependence-Based Risk Decomposition (Kendall's τ)

Assets	$R_{i,S}^{\tau}$	$R_{i,M\|S}^{\tau}$	$R_{i,\varepsilon}^{\tau}$	Total
$r_{1,t}^{F}$	58.87%	21.97%	19.16%	100%
$r_{2,t}^{F}$	60.95%	14.46%	24.59%	100%
$r_{1,t}^{E}$	80.54%	4.45%	15.01%	100%
$r_{2,t}^{E}$	70.41%	9.88%	19.71%	100%

To assess robustness, a sensitivity analysis based on lower and upper tail dependence coefficients was conducted, as reported in Table 6. The results showed that sectoral dependence dominated in the upper tail for all assets, whereas lower-tail dependence exhibited greater variation. In particular, BBRI and PGAS showed substantial conditional market contributions under adverse market conditions, indicating stronger market effects during extreme negative events. The non-systematic component was negligible in the tail-based decomposition due to the Gaussian specification in higher-order trees, which does not exhibit tail dependence.

Table 6. Sensitivity Analysis Using Tail Dependence (λ)

Assets	$R_{i,S}^{\lambda_L}$	$R_{i,M\|S}^{\lambda_L}$	$R_{i,\varepsilon}^{\lambda_L}$	$R_{i,S}^{\lambda_U}$	$R_{i,M\|S}^{\lambda_U}$	$R_{i,\varepsilon}^{\lambda_U}$
$r_{1,t}^{F}$	100%	0%	0%	100%	0%	0%
$r_{2,t}^{F}$	61.25%	38.75%	0%	100%	0%	0%
$r_{1,t}^{E}$	100%	0%	0%	100%	0%	0%
$r_{2,t}^{E}$	50.32%	49.68%	0%	100%	0%	0%

Overall, the consistency between the τ-based and λ-based decompositions supported the robustness of the dependence-based allocation. Sectoral effects dominated under normal conditions, whereas conditional market dependence became more pronounced in the lower tail during extreme negative market movements. These findings also provided a basis for portfolio optimization under tail-risk considerations.

To incorporate the estimated dependence structure into the optimization process, return simulations were generated using the fitted RVMS model. The simulated returns preserved the nonlinear and hierarchical dependence structure captured by the copula model, allowing a more realistic representation of joint asset behavior under extreme market conditions. These simulated returns were subsequently used to estimate Value-at-Risk (VaR) and Expected Shortfall (ES) for portfolio optimization.

3.6 Portfolio Optimization

Portfolio optimization was performed using the minimum CVaR criterion at the 95% and 99% confidence levels for a four-asset portfolio consisting of BBCA, BBRI, ADRO, and PGAS. Table 7 presents the resulting portfolio weights under the RVMS and CAPM frameworks.

Table 7. Portfolio Assets Weights from RVMS and CAPM

Model	α	$r_{1,t}^{F}$	$r_{2,t}^{F}$	$r_{1,t}^{E}$	$r_{2,t}^{E}$	VaR	CVaR	SE	95%CI
RVMS	95%	40%	29.65%	15.85%	14.49%	-0.020	-0.0288	0.0008	(-0.031,-0.027)
	99%	40%	31.26%	12.42%	16.32%	-0.034	-0.0444	0.0023	(-0.049,-0.040)
CAPM	95%	40%	10%	10%	40%	-0.021	-0.0329	0.0041	(-0.041,-0.025)
	99%	40%	10%	10%	40%	-0.038	-0.0523	0.0115	(-0.076,-0.036)

At both confidence levels, RVMS produced less negative CVaR values than CAPM, indicating lower expected tail losses, particularly at the 99% level. RVMS also generated smaller standard errors and narrower 95% confidence intervals, suggesting more stable tail-risk estimates. In contrast, CAPM exhibited greater sensitivity to sampling variability under extreme conditions.

Overall, while RVMS improved statistical risk performance through lower CVaR and more stable risk estimates, this did not necessarily imply superior economic performance. Therefore, additional metrics such as the Sharpe ratio, maximum drawdown, and portfolio turnover were also evaluated to assess practical portfolio performance.

3.7 Backtesting Model

The evaluation results are divided into two dimensions: statistical risk accuracy and economic performance. Statistical accuracy is assessed using Kupiec, Christoffersen, and McNeil-Frey tests, while economic value is evaluated through Sharpe ratio, maximum drawdown, and portfolio turnover. This distinction is important, as improvements in statistical risk modeling do not necessarily translate into better portfolio performance.

3.7.1 Statistical Risk

The backtesting results for the CAPM and RVMS models at the 95% and 99% confidence levels are presented in Table 8.

Table 8. Statistical Risk Results

Model	α	Expected	Actual	Kupiec (p-value)	Christoffersen (p-value)	McNeil-Frey
RVMS	95%	33	38	Accept (0.467)	Accept (0.365)	Accept (0.105)
CAPM	95%	33	43	Accept (0.121)	Accept (0.116)	Reject (0.025)
RVMS	99%	6	11	Accept (0.133)	Reject (0.012)	Accept (0.802)
CAPM	99%	6	16	Reject (0.002)	Reject (0.002)	Accept (0.067)

At the 95% confidence level, both models passed the Kupiec and Christoffersen tests, indicating adequate unconditional and conditional coverage. However, the McNeil–Frey test rejected the CAPM model, suggesting underestimation of tail losses, whereas RVMS provided more accurate tail-risk estimates. At the 99% confidence level, both models fail to satisfy the coverage requirements. The CAPM model is rejected under both the Kupiec and Christoffersen tests, indicating significant underestimation and violation clustering. The RVMS model shows partial improvement by passing the unconditional coverage test but still failing the conditional coverage test, indicating remaining dependence in violation occurrences. This was confirmed by the estimated transition probabilities, $P = (V_t = 1|V_{t-1} = 0) = 0$ and $P = (V_t = 1|V_{t-1} = 1) = 1$, which showed that violations occurred in consecutive clusters rather than independently. The violation indicator plot in Figure 4 also showed clustering during periods of market stress, explaining the rejection of the conditional coverage test and highlighting the difficulty of modeling extreme tail dependence.

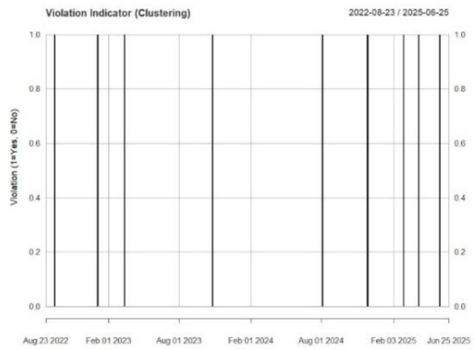

Figure 4. Plot Violation Clustering RVMS

To further assess the reliability of the model under extreme conditions, bootstrap confidence intervals were constructed too for the VaR estimates under the RVMS model at the 99% confidence level. The resulting interval [-0.0393, -0.0280] were relatively wide, indicating substantial uncertainty in extreme quantile estimation.

3.7.2 Economic Performance

In addition to statistical risk accuracy, it is important to evaluate whether the proposed model provides tangible benefits from a portfolio management perspective. Table 9 compares the economic performance of the RVMS and CAPM portfolios. All portfolios exhibited negative Sharpe ratios, indicating that neither model achieved positive risk-adjusted returns during the evaluation period. Nevertheless, RVMS consistently produced higher (less negative) Sharpe ratios and lower maximum drawdowns than CAPM, particularly at the 99% confidence level, indicating modest improvements in downside risk control.

Table 9. Economic Performance Comparison

Model	α	Sharpe Ratio	Max Drawdown	Turnover
RVMS	95%	-0.547	0.385	0.098
CAPM	95%	-0.568	0.393	0.026
RVMS	99%	-0. 506	0.360	0.054
CAPM	99%	-0.568	0.379	0.062

Although RVMS exhibited higher turnover, implying more active rebalancing, turnover declined at the 99% confidence level, suggesting more stable allocations under stronger tail-risk considerations. Overall, the economic improvements of RVMS remained moderate.

4. CONCLUSION

This study evaluated the RVMS framework as a sector-conditioned extension of CAPM for portfolio risk optimization. The results showed that RVMS improved downside risk estimation at standard confidence levels, reducing expected tail losses by approximately 12–16%. However, this advantage weakened under more extreme conditions, highlighting the continuing challenge of modeling extreme tail risk.

RVMS also provided modest improvements in risk-adjusted performance and lower drawdowns, although these benefits were accompanied by higher portfolio turnover, implying more active rebalancing. Methodologically, the findings demonstrated that incorporating sector-conditioned hierarchical dependence extends beyond single-factor representations by allowing heterogeneous dependence patterns across assets. Nevertheless, the improvements remained moderate and context-dependent.

These conclusions are limited to the analyzed assets, sample period, and model specifications. In particular, the static dependence structure and simplified higher-order vine assumptions may reduce the model's ability to capture rapidly changing market conditions. Future studies should consider time-varying dependence structures, broader asset universes, and transaction costs to further evaluate practical applicability.

5. REFERENCES

[1] E. Sommer, K. Bax, and C. Czado, "Vine copula based portfolio level conditional risk measure forecasting," *Econom. Stat.*, 2023. [Online]. Available: https://doi.org/10.1016/j.ecosta.2023.08.002

[2] Y. P. Putra, H. Setiorini, and C. Suhendra, "Analisis keakuratan capital asset pricing model dan arbitrage pricing theory dalam memprediksi return saham (studi pada perusahaan LQ 45 di bursa efek Indonesia periode 2016-2020)," *J. Ilm. Ekon. dan Bisnis*, vol. 11, no. 1, pp. 839–848, 2023. [Online]. Available: https://doi.org/10.37676/ekombis.v11i1.3254

[3] W. F. Sharpe, "Capital asset prices: a theory of market equilibrium under conditions of risk," *J. Finance*, vol. 19, no. 3, pp. 425–442, 1964. [Online]. Available: https://doi.org/10.1111/j.1540-6261.1964.tb02865.x

[4] E. F. Fama and K. R. French, "The capital asset pricing model: theory and evidence," *J. Econ. Perspect.*, vol. 18, no. 3, pp. 25–46, 2004. [Online]. Available: https://doi.org/10.1257/0895330042162430.

[5] E. C. Brechmann and C. Czado, "Risk management with high-dimensional vine copulas: an analysis of the Euro Stoxx 50," *Stat. Risk Model.*, vol. 30, no. 4, pp. 307–342, 2013. [Online]. Available: https://doi.org/10.1524/strm.2013.2002

[6] A. Asthana, S. Shafi, and A. Tiwari, "Empirical evidence on the validity of the conditional higher moment CAPM in the Bombay Stock Exchange," *J. Econ. Manag. Trade*, vol. 30, no. 4, pp. 37–45, 2024. [Online]. Available: https://doi.org/10.9734/JEMT/2024/v30i41203

[7] M. Galea, D. Cademartori, R. Curci, and A. Molina, "Robust inference in the capital asset pricing model using the multivariate t -distribution," *J. Risk Financ. Manag*, vol. 13, no. 6, pp. 1–22, 2020. [Online]. Available: https://doi.org/10.3390/jrfm13060123

[8] A. Wibowo and S. Darmanto, "Empirical test of the capital asset pricing model (CAPM): evidence from Indonesia capital market," *Int. J. Econ. Manag. Stud.*, vol. 7, no. 5, pp. 180–185, 2020. [Online]. Available: https://doi.org/10.14445/23939125/ijems-v7i5p126

[9] H. Jiang, "Capital asset pricing model and its application on investment risk," *Highlights Business, Econ. Manag.*, vol. 45, pp. 300–306, 2024. [Online]. Available: https://doi.org/10.54097/f832wg56

[10] C. Özgür and V. Sarıkovanlık, "An application of regular vine copula in portfolio risk forecasting: evidence from Istanbul stock exchange," *Quant. Financ. Econ.*, vol. 5, no. 3, pp. 452–470, 2021. [Online]. Available: https://doi.org/10.3934/qfe.2021020

[11] A. Khairiati, R. Budiarti, and I. G. P. Purnaba, "Perbandingan analisis regresi linear dengan analisis regresi copula pada data keuangan," *Jambura J. Math.*, vol. 4, no. 2, pp. 209–219, 2022. [Online]. Available: https://doi.org/10.34312/jjom.v4i2.13829

[12] E. Ivanov, A. Min, and F. Ramsauer, "Copula-based factor models for multivariate asset returns," *Econometrics*, vol. 5, no. 2006, pp. 1–24, 2017. [Online]. Available: https://doi.org/10.3390/econometrics5020020

[13] A. J. Patton, *Copula Methods for Forecasting Multivariate Time Series*, vol. 2 Part B. Elsevier, 2013. [Online]. Available: https://doi.org/10.1016/B978-0-444-62731-5.00016-6

[14] B. Tim and R. M. Cooke, "Vines — a new graphical model for dependent random variables," *Ann. Stat.*, vol. 30, no. 4, pp. 1031–1068, 2002. [Online]. Available: https://doi.org/10.1214/aos/1031689016

[15] K. Aas, C. Czado, A. Frigessi, and H. Bakken, "Pair-copula constructions of multiple dependence," *Insur. Math. Econ.*, vol. 44, no. 2, pp. 182–198, 2009. [Online]. Available: https://doi.org/10.1016/j.insmatheco.2007.02.001

[16] T. Nagler and C. Czado, "Evading the curse of dimensionality in nonparametric density estimation with simplified vine copulas," *J. Multivar. Anal.*, vol. 151, pp. 69–89, 2016. [Online]. Available: https://doi.org/10.1016/j.jmva.2016.07.003

[17] M. Sahamkhadam and A. Stephan, "Portfolio optimization based on forecasting models using vine copulas : An empirical assessment for the global financial and for the COVID-19 crisis," *J. Forecast.*, vol. 42, no. 8 December 2023, pp. 2139–2166, 2023. [Online]. Available: https://doi.org/10.1002/for.3009

[18] R. Bedoui, S. Noiali, H. Hamdi, "Hedge funds portfolio optimization using vine copula-GARCH-EVT-CVaR model," *Int. J. Entrep. Small Business, Inderscience Enterp. Ltd*, vol. 39, no. 1–2, pp. 121–148, 2020. [Online]. Available: https://doi.org/10.1504/IJESB.2020.104247

[19] R. Bedoui *et al.*, "Portfolio optimization through hybrid deep learning and genetic algorithms vine copula-GARCH-EVT-CVaR Model," *Technol. Forecast. Soc. Change*, vol. 197, p. 122887, 2023. [Online]. Available: https://doi.org/10.1016/j.techfore.2023.122887

[20] I. N. Kyalo, C. O. Omari, and A. Ngunyi, "Optimization of financial asset portfolio using GARCH-EVT-copula-CVaR Model," *J. Math. Financ.*, vol. 15, no. 03, pp. 579–615, 2025. [Online]. Available: https://doi.org/10.4236/jmf.2025.153024.

[21] A. Heinen, A. Valdesogo, "Asymmetric CAPM dependence for large dimensions : the canonical vine autoregressive model," *SSRN*, 2009. [Online]. Available: https://doi.org/10.2139/ssrn.1297506

[22] O. Evkaya, İ. Gür, B. Yıldırım, and G. Poyraz, "Vine copula approach to understand the financial dependence of the Istanbul stock exchange index," *Comput. Econ. Springer*, vol. 64, no. 5, pp. 2935–2980, 2024. [Online]. Available: https://doi.org/10.1007/s10614-023-10544-7

[23] T. Chaiyawat and P. Guayjarernpanishk, "Enhancing insurer portfolio resilience and capital efficiency with green bonds: a framework combining dynamic r-vine copulas and tail-risk modeling," *Risks*, vol. 13, no. 9, pp. 1–34, 2025. [Online]. Available: https://doi.org/10.3390/risks13090163

[24] E. N. Damayanti and H. Kuswanto, "Analisis risiko pada return saham perusahaan asuransi menggunakan metode VaR dengan pendekatan ARMA-GARCH," *J. Mat. Stat. dan Komputasi*, vol. 16, no. 1, pp. 40–50, 2019. [Online]. Available: https://doi.org/10.20956/jmsk.v16i1.6197

[25] R. Budiarti, K. Intansari, I. G. P. Purnaba, and F. Septyanto, "Modelling dependencies of stock indices during covid-19 pandemic by extreme-value copula," *JTAM*, vol. 7, no. 3, pp. 805–819, 2023. [Online]. Available: https://doi.org/10.31764/jtam.v7i3.15109

[26] D. B. B. Nguyen, M. Prokopczuk, and P. Sibbertsen, "The memory of stock return volatility : asset pricing implication," *J. Financ. Mark. Forthcom.*, vol. 47, no. C, 2020. [Online]. Available: https://doi.org/10.1016/j.finmar.2019.01.002

[27] E. M. Kimani, A. Ngunyi, and J. K. Mungatu, "Modelling dependence of cryptocurrencies using copula GARCH," *J. Math. Financ.*, vol. 13, pp. 321–338, 2023. [Online]. Available: https://doi.org/10.4236/jmf.2023.133020

[28] H. Joe, H. Li, and A. K. Nikoloulopoulos, "Tail dependence functions and vine copulas," *J. Multivar. Anal.*, vol. 101, no. 1, pp. 252–270, 2010. [Online]. Available: https://doi.org/10.1016/j.jmva.2009.08.002

[29] C. Czado and T. Nagler, "Vine copula based modeling," *Annu. Rev. Stat. Its Appl.*, vol. 9, pp. 453–477, 2022. [Online]. Available: https://doi.org/10.1146/annurev-statistics-040220-101153

[30] M. Gulliksson, S. Mazur, and A. Oleynik, "Results in applied mathematics minimum VaR and minimum CVaR optimal portfolios : the case of singular covariance matrix," *Results Appl. Math.*, vol. 26, p. 100557, 2025. [Online]. Available: https://doi.org/10.1016/j.rinam.2025.100557

[31] M. Sahamkhadam, A. Stephan, and R. Östermark, "Copula-based black – litterman portfolio optimization," *Eur. J. Oper. Res.*, vol. 297, no. 3, pp. 1055–1070, 2022. [Online]. Available: https://doi.org/10.1016/j.ejor.2021.06.015

[32] R. T. Rockafellar and S. Uryasev, "Optimization of conditional value-at-risk," *J. Risk*, vol. 2, no. 3, pp. 21–41, 2000. [Online]. Available: https://doi.org/10.21314/JOR.2000.038

[33] P. F. Christoffersen, "Evaluating interval forecasts," *Int. Econ. Rev. (Philadelphia).*, vol. 39, no. 4, pp. 841–862, 1998. [Online]. Available: https://doi.org/10.2307/2527341

[34] A. J. McNeil and R. Frey "Estimation of tail-related risk measures for heteroscedastic financial time series: an extreme value approach," *J. Empir. Financ.*, vol. 7, no. 3–4, pp. 271–300, 2000. [Online]. Available: https://doi.org/10.1016/S0927-5398(00)00012-8